

Stability of plant immune-receptor resistance proteins is controlled by SKP1-CULLIN1-F-box (SCF)-mediated protein degradation

Yu Ti Cheng^a, Yingzhong Li^b, Shuai Huang^{a,c}, Yan Huang^{a,c}, Xinnian Dong^d, Yuelin Zhang^b, and Xin Li^{a,c,1}

^aMichael Smith Laboratories, and ^cDepartment of Botany, University of British Columbia, Vancouver, BC, Canada V6T 1Z4; ^bNational Institute of Biological Sciences, Beijing 102206, People's Republic of China; and ^dDepartment of Biology, Duke University, Durham, NC 27708

Edited by Paul Schulze-Lefert, The Max Planck Institute for Plant Breeding Research, Cologne, Germany, and approved August 3, 2011 (received for review April 12, 2011)

The nucleotide-binding domain and leucine-rich repeats containing proteins (NLRs) serve as immune receptors in both plants and animals. Overaccumulation of NLRs often leads to autoimmune responses, suggesting that the levels of these immune receptors must be tightly controlled. However, the mechanism by which NLR protein levels are regulated is unknown. Here we report that the F-box protein CPR1 controls the stability of plant NLR resistance proteins. Loss-of-function mutations in *CPR1* lead to higher accumulation of the NLR proteins *SNC1* and *RPS2*, as well as autoactivation of immune responses. The autoimmune responses in *cpr1* mutant plants can be largely suppressed by knocking out *SNC1*. Furthermore, *CPR1* interacts with *SNC1* and *RPS2* in vivo, and overexpressing *CPR1* results in reduced accumulation of *SNC1* and *RPS2*, as well as suppression of immunity mediated by these two NLR proteins. Our data suggest that SKP1-CULLIN1-F-box (SCF) complex-mediated stability control of plant NLR proteins plays an important role in regulating their protein levels and preventing autoimmunity.

Plants and animals rely on innate immunity to defend against microbial pathogen infections. Although plant surface-residing receptors often recognize common features of the microbes, intracellular receptors detect specific effectors from pathogens to initiate a downstream defense cascade (1). Remarkably, plants and animals use immune sensors with similar structural features, such as nucleotide-binding (NB) and leucine-rich repeats (LRR) domains (2). These immune receptors are commonly named Nod-like Receptors (NLRs; or nucleotide-binding and leucine-rich repeat-containing) after the human innate immunity receptor Nod1 and Nod2 (3). In plants, they are designated as NB-LRR resistance proteins (NLR R proteins). Upon detection of specific pathogen effectors, R proteins mount a quick and robust reaction, usually culminating in a hypersensitive response, a type of programmed cell death, to defend against and restrict further spread of the pathogen (1). Because of the detrimental effects of R protein activation on plant cell growth and development, normally R protein-mediated immunity has to be under multiple levels of tight negative control. Overaccumulation of R proteins often leads to autoimmunity, implying the importance of stability control of R protein levels. In addition, gain-of-function mutants of NLRs, such as *sncl* (*suppressor of npr1-1, constitutive 1*) and *ssi4* (*suppressor of salicylic acid insensitivity of npr1-5, 4*), can render the NLR proteins constitutively active without pathogen interaction (4, 5). These mutations are speculated to enhance the stability or activities of the NLRs. Constitutive expression of defense marker *Pathogenesis Related (PR)* genes, enhanced pathogen resistance, and altered plant development, such as dwarfism, are general features of plant autoimmunity.

The *Arabidopsis* genome contains about 170 genes encoding NLRs (6), with either Toll/IL-1 receptor (TIR) or coiled-coil (CC) domains at their N terminus. The detailed activation mechanism of NLR R proteins is unclear. During the past decade, intensive studies on RAR1, SGT1, and HSP90 using genetic and biochemical approaches established these components as members of

a protein complex required for chaperone activities to properly fold and stabilize NLR R proteins (7, 8). Interestingly, mammalian SGT1 and HSP90 were also shown to be required for NLR-mediated immune responses. Some NLRs, including Nod1 and Nod2, form complexes with HSP90 and SGT1 (9).

Aside from the positive roles SGT1 plays in R protein folding, it is also involved in the negative regulation of R protein stability. A loss-of-function mutation in *SGT1b* restores reduced accumulation of CC-type NLR RPS5 in *rar1* mutant plants (10). In addition, accumulation of *SNC1* is increased in *sgt1b* mutant plants. Recently, the evolutionarily conserved SRF1 was shown to interact directly with SGT1 (11). Loss-of-function of *SRFR1* results in increased accumulation of *SNC1* and activation of *SNC1*-mediated defense responses (11, 12). However, the mechanism on how SGT1 and SRF1 negatively regulate the accumulation of R proteins is unclear.

Besides interactions with HSP90 and RAR1, SGT1 was also shown to associate with SKP1 and CULLIN1 (*CUL1*) (7, 13), members of the SCF (SKP1-CUL1-F-box protein) E3 ubiquitin ligase complex that targets specific substrate proteins for ubiquitination and most often subsequent protein degradation. The F-box protein usually interacts directly with the protein substrate and serves as the substrate determinant of SCF. The association between SGT1 and SCF suggests potential connections between SCF and R protein-mediated immunity. Here we provide experimental evidence that *Arabidopsis* F-box protein CPR30/CPR1 targets NLR proteins *SNC1* and *RPS2* for degradation, revealing how some NLR R protein levels are controlled mechanistically.

Results

***sncl* Mutation Affects the Stability of *SNC1*.** The gain-of-function mutant *sncl* carries a mutation in *SNC1*, an NLR R-like gene that leads to constitutive activation of defense responses in *Arabidopsis* (4, 14). Like other TIR-type R proteins, *sncl* signals through *PAD4* (15). Mutations in *PAD4* can completely suppress the dwarfism of *sncl* caused by autoimmunity (Fig. 1A). To investigate how the E552 to K552 change in the linker region causes constitutive activation of *SNC1*, we first examined the *sncl* transcript level in the mutant and found only a moderate increase (Fig. 1B). This increase is fully suppressed when *PAD4*, an essential signaling component downstream of *SNC1*, is mutated (Fig. 1B), indicating that the increased *sncl* transcription is caused by feedback up-regulation from downstream defense signaling. With the availability of an antibody specific to the endogenous *SNC1* protein (11), we analyzed *sncl* protein levels

Author contributions: Y.T.C., Y.L., Y.Z., and X.L. designed research; Y.T.C., Y.L., and S.H. performed research; Y.Z. and X.L. contributed new reagents/analytic tools; Y.T.C., Y.L., S.H., Y.H., X.D., Y.Z., and X.L. analyzed data; and Y.T.C., X.D., Y.Z., and X.L. wrote the paper.

The authors declare no conflict of interest.

This article is a PNAS Direct Submission.

¹To whom correspondence should be addressed. E-mail: xinli@interchange.ubc.ca.

This article contains supporting information online at www.pnas.org/lookup/suppl/doi:10.1073/pnas.1105685108/-DCSupplemental.

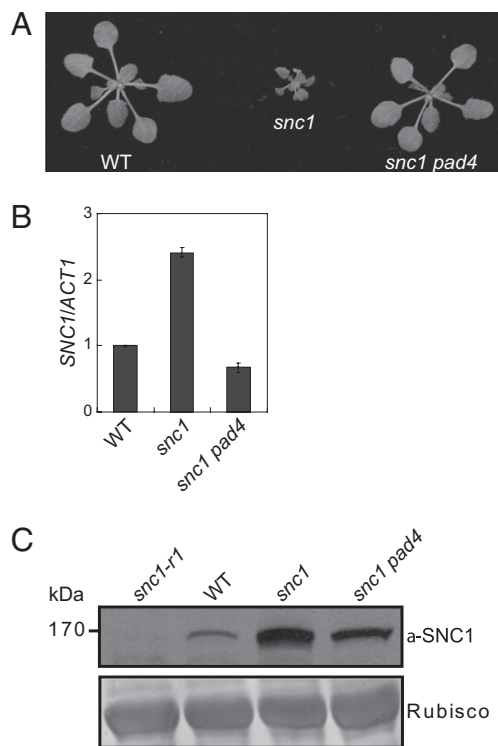


Fig. 1. Increased *sncl* protein levels in *sncl* and *sncl pad4* double mutant. (A) Morphology of wild-type Col (WT), *sncl* (gain-of-function allele of *SNC1*), and *sncl pad4* double-mutant plants (14). The picture was taken with 4-wk-old soil-grown plants. (B) qRT-PCR analysis of *SNC1* transcript levels in WT, *sncl*, and *sncl pad4* plants. (C) Western blot analysis of *SNC1*/*sncl* protein levels in *sncl-r1* (a loss-of-function deletion allele of *SNC1*), WT, *sncl*, and *sncl pad4* plants (14). Rubisco levels serve as loading control.

in *sncl* and *sncl pad4* plants. To our surprise, *sncl* protein levels are still considerably higher in the *sncl pad4* double-mutant plants than that in the wild-type (Fig. 1C), suggesting that the *sncl* mutation renders the R protein more stable.

***cull1-7* Exhibits Increased *SNC1* Level and Constitutive Defense Responses.** Because a mutation in *SGT1b* also results in increased *SNC1* protein level and *SGT1* associates with *SKP1* and *CUL1* (7, 11, 13), two shared members of the SCF E3 ubiquitin ligase complex, we asked whether the stability of *SNC1* could be controlled by SCF-mediated protein degradation. In *Arabidopsis*, null mutations in *CUL1* are lethal (16). A partial loss-of-function allele of *CUL1*, *cull1-7*, was found to exhibit a dwarf phenotype similar to *sncl* (17) (Fig. 2A). In *cull1-7*, the T510 to I510 substitution seems to affect the C terminus of the protein, as well as the stability of *CUL1*, thus resulting in the misregulation of SCFs. The mutant exhibited accumulation of target proteins of many known SCF complexes, including *AUS/IAA1* and *RGA1* for auxin and gibberellic acid signaling, respectively (17). Additionally, *cull1-7* plants express high levels of defense-marker *PR* genes, *PR1* and *PR2* (Fig. 2B and C), suggesting that the mutation causes activation of defense responses. The dwarfism of *cull1-7* is more severe than that of *sncl* and can be partially complemented by a transgene expressing the *CUL1-FLAG* fusion protein (17) (Fig. 2A). Although the transcript level of *SNC1* in *cull1-7* is not significantly different from that of wild-type (Fig. 2D), Western blot analysis showed that the *SNC1* protein level in *cull1-7* was much higher than that in wild-type and this increased accumulation of *SNC1* can be partially complemented by the *CUL1-FLAG* transgene (Fig. 2E), indicating that *CUL1* contributes to the control of *SNC1* levels. Furthermore, quantitative RT-PCR analysis of a variety of known *R* genes indicates

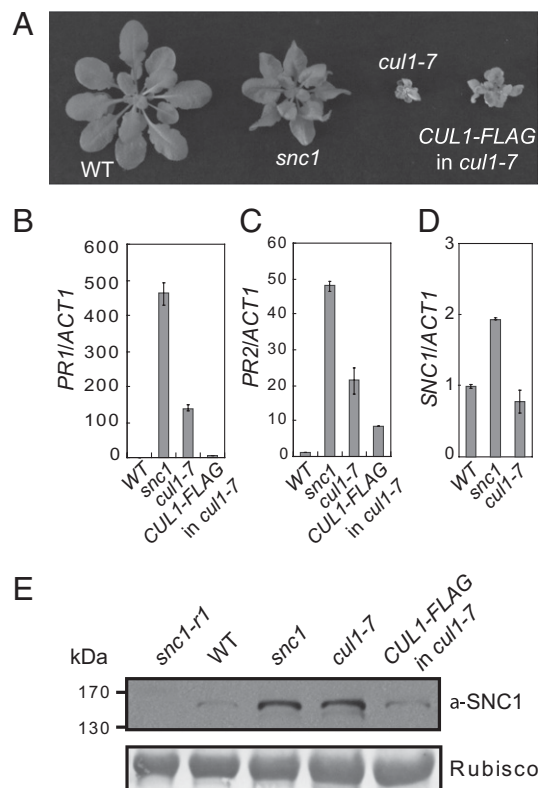


Fig. 2. Increased accumulation of *SNC1* protein levels in *cull1-7* mutant. (A) Morphology of WT, *sncl*, *cull1-7*, and *cull1-7* carrying the partially complementing transgene *CUL1-FLAG* (*CUL1-FLAG* in *cull1-7*) (17). The picture was taken with 5-wk-old soil-grown plants. (B–D) qRT-PCR analysis of the expression of *PR1* (B), *PR2* (C), and *SNC1* (D) in the indicated genotypes. (E) Western blot analysis of *SNC1*/*sncl* protein levels in *sncl-r1* (a loss-of-function deletion allele of *SNC1*), WT, *sncl*, *cull1-7*, and *CUL1-FLAG* in *cull1-7*.

that transcript levels of these *R* genes are not significantly increased in *cull1-7* (Fig. S1), suggesting that SCF-mediated protein ubiquitination has little effect on *R* gene transcription.

***SNC1* Protein Levels Are Increased in *cpr1* and *cpr30* Mutants.** The substrate specificity of the SCF complexes is most often determined by the F-box proteins. Previously it was shown that mutations in the F-box protein, *CPR30* [At4g12560; Constitutive *PR* gene expression, 30 (*cpr30*)], lead to constitutive activation of *PR* genes, accumulation of the defense hormone salicylic acid, and a dwarf phenotype strikingly similar to that of *sncl* (18) (Fig. S2). Western blot analysis revealed that *SNC1* overaccumulates in the *cpr30* mutant plants (Fig. 3A). Another well-known mutant with constitutive defense responses and *sncl*-like morphology is *cpr1* (19) (Fig. 3B and Fig. S2). Although *cpr1* was isolated over 15 y ago, its identity was unknown. Interestingly, similar to the *cpr30* alleles, the *SNC1* protein level in *cpr1* was much higher than that in wild-type (Fig. 3A). The levels of *SNC1* in *cpr1* and two alleles of *cpr30* are very similar. To exclude the possibility that *CPR1* negatively controls *SNC1* expression, we checked the *SNC1* expression level in *cpr1* and *cpr1 pad4* mutants. As shown in Fig. S3A, *SNC1* transcript level is only slightly increased in *cpr1* and this increase is completely reverted by *pad4* in the *cpr1 pad4* double mutant, suggesting that the small increase of *SNC1* transcription is caused by feedback up-regulation from downstream defense signaling. In contrast, *SNC1* levels in the *cpr1 pad4* double mutants remain much higher than in wild-type and not drastically reduced from that in *cpr1* (Fig. S3B), confirming that *CPR1* negatively regulates *SNC1* protein level. Interestingly, *SNC1* levels in *cpr30* and *cpr30 pad4* are also much higher than that in wild-type (Fig. S3B). Fur-

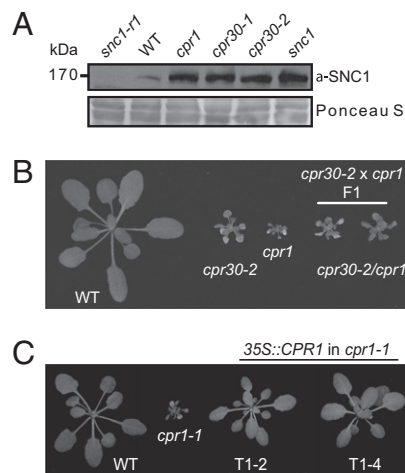


Fig. 3. Both *cpr1* and *cpr30* are alleles of *At4g12560*. (A) Western blot analysis of SNC1 protein levels in *cpr1* (renamed *cpr1-1*), *cpr30-1* (renamed *cpr1-2*), and *cpr30-2* (renamed *cpr1-3*). *snc1-r1* (a loss-of-function deletion allele of *SNC1*), WT, and *snc1* plants were used as controls. (B) Allelism test between *cpr30-2* and *cpr1*. Morphology of two F1 plants from the cross between *cpr30-2* and *cpr1*, with WT, *cpr30-2*, and *cpr1* plants as controls. (C) Complementation of *cpr1-1* by the *CPR1* transgene under 35S promoter. Morphologies of two independent transgenic lines (T1-2 and T1-4) are shown.

Furthermore, quantitative RT-PCR analysis of several other *R* genes indicates that their transcript levels are not drastically increased in *cpr1* or *cpr1 pad4* (Fig. S3 C–I), suggesting that CPR1 has little effect on *R* gene transcription.

***cpr1* and *cpr30* Are Allelic Mutations.** Because *cpr1* and *cpr30* are both recessive mutations mapped to chromosome 4 (18, 19), we crossed *cpr1* and *cpr30-2* to test for allelism. As shown in Fig. 3B, *cpr1* and *cpr30-2* failed to complement in F1, indicating that they are allelic to each other. Because *cpr1* was identified as the founding member of the *cpr*-type mutants, for simplicity and to avoid confusion in the literature, we renamed *cpr1* as *cpr1-1*, the allele obtained by Gou et al. (18) (previously named *cpr30-1*) as *cpr1-2*, and the T-DNA allele (SALK_045148; previously named *cpr30-2*) as *cpr1-3*. Further sequence analysis of *cpr1-1* revealed a G to A point mutation in *At4g12560*. This mutation is located at an intron-exon junction (Fig. S4), leading to a shift of the splicing site which results in a reading frame change in the gene. When a construct expressing *At4g12560* under the control of a 35S promoter was transformed into *cpr1-1*, all transgenic plants exhibited wild-type morphology (Fig. 3C); this confirms that the *cpr1-1* mutant phenotype was caused by the mutation in *At4g12560*. Phylogenetic analysis of CPR1 and its homologs indicates that they are also present in other higher plants (Fig. S5).

Constitutive Defense Responses in *cpr1-3* Are Largely Suppressed by Knocking Out *SNC1*. To test whether the increased SNC1 protein accumulation contributes to the activation of defense responses in the *cpr1* mutants, we crossed *snc1-r1*, a loss-of-function deletion allele of *SNC1* (14), into *cpr1-3*. As shown in Fig. 4A, the *snc1-r1* mutation reverted *cpr1-3* to wild-type morphology. Analysis of *PR* gene expression showed that constitutive expression of both *PR1* and *PR2* was reduced in *snc1-r1 cpr1-3* (Fig. 4B and C). In addition, enhanced resistance against the virulent oomycete pathogen *Hyaloperonospora arabidopsidis* Noco2 in *cpr1-3* was also attenuated by the *snc1-r1* mutation (Fig. 4D). These data suggest that overaccumulation of SNC1 in *cpr1-3* is one of the main factors leading to the *cpr1* autoimmune mutant phenotypes.

Overexpression of CPR1 Results in Reduced *snc1* Protein Levels and Suppression of *snc1* Mutant Phenotypes. Increased accumulation of SNC1 protein in *cpr1* mutants and suppression of *cpr1-3* phe-

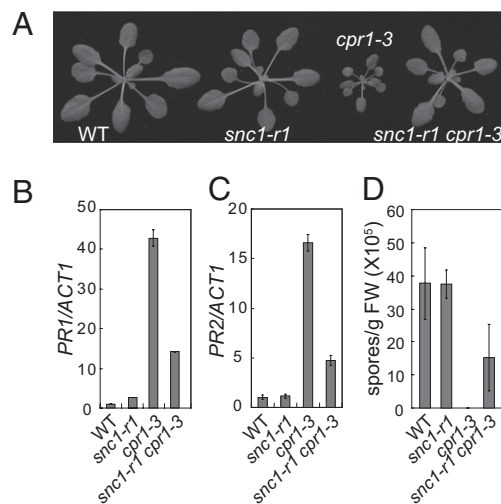


Fig. 4. CPR1 regulates SNC1-mediated defense responses. (A) Morphology of WT, *snc1-r1* (a loss-of-function deletion allele of *SNC1*), *cpr1-3*, and *snc1-r1 cpr1-3* mutant plants. (B and C) qRT-PCR analysis of *PR1* (B) and *PR2* (C) expression in *snc1-r1*, *cpr1-3*, and *snc1-r1 cpr1-3*. (D) Growth of *H. arabidopsidis* Noco2 spores on the indicated genotypes.

notypes by *snc1-r1* suggest that CPR1 might target SNC1 for degradation. Because the F-box proteins are usually the limiting factor in SCF-mediated target protein degradation, we tested whether overexpression of *CPR1* would reduce the accumulation of SNC1 by overexpressing *CPR1* in the *snc1* mutant background. As shown in Fig. 5A, *snc1* transgenic lines T1-5 and T1-6 carrying 35S::*CPR1* exhibit wild type-like morphology. Both lines expressed high levels of *CPR1* (Fig. S6A) and modestly reduced level of *SNC1* (Fig. S6B) because of reduced feedback up-reg-

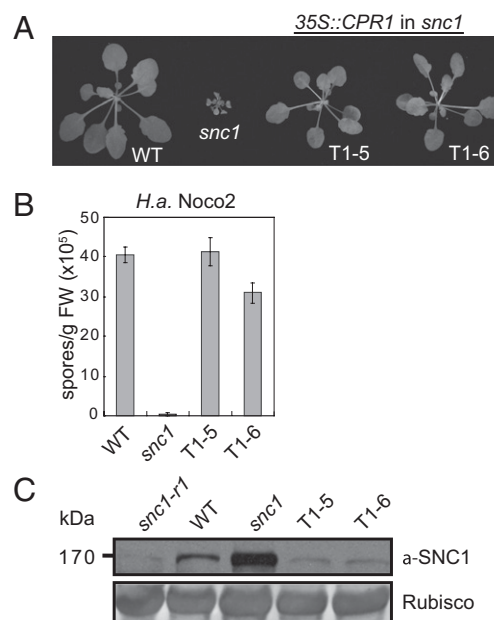


Fig. 5. Overexpression of *CPR1* in *snc1* alleviates the enhanced disease resistance phenotypes of *snc1* and reduces the protein levels of *snc1*. (A) Morphology of WT, *snc1*, and two independent transgenic lines (T1-5 and T1-6) overexpressing *CPR1* in the *snc1* mutant background. (B) Growth of *H. arabidopsidis* Noco2 spores on the indicated genotypes. (C) Western blot analysis of *snc1*/*SNC1* protein levels in the transgenic lines over-expressing *CPR1*. *snc1-r1*, WT, and *snc1* plants were used as controls.

ulation in *snc1*. In addition, enhanced resistance against *H. arabidopsidis* Noco2 (Fig. 5B) and constitutive *PR* gene expression (Fig. S6 C and D) in *snc1* were completely suppressed in the *CPR1* overexpression lines. Western blot analysis revealed that *snc1* protein accumulation was clearly reduced even below the wild-type level in the two *CPR1* overexpression lines (Fig. 5C). These data support that *CPR1* is the F-box protein targeting *SNC1* for degradation.

Overexpression of *CPR1* Affects R Protein-Mediated Resistance. Although *snc1-r1* completely suppresses the dwarfism of *cpr1-3*, constitutive *PR* gene expression and enhanced resistance against *H. arabidopsidis* Noco2 in *cpr1-3* is only partially attenuated by *snc1-r1* (Fig. 4 B–D), suggesting that *CPR1* may also target R proteins other than *SNC1* for degradation. The residual enhanced resistance in *snc1-r1 cpr1-3* is probably caused by increased accumulation of the other R proteins. To test this hypothesis, we generated transgenic lines overexpressing *CPR1* in the wild-type Columbia (WT) background (Fig. S7A) and challenged the transgenic plants with pathogens carrying different effectors that activate specific R protein-mediated resistance. The two *CPR1* overexpression lines were slightly more susceptible to the virulent bacterial pathogen *Pseudomonas syringae* pv. *tomato* DC3000 (Fig. 6A). In contrast, resistance mediated by *RPS2* and *RPM1* is severely compromised when *CPR1* is expressed at high levels (Fig. 6B and Fig. S7B), suggesting that *CPR1* may also target R proteins, such as *RPS2* and *RPM1*, for degradation. Because the expression levels of *RPS2* and *RPM1* are not significantly affected in these transgenic plants, the defects in *RPS2*- and *RPM1*-mediated resistance in *CPR1* overexpressing lines are not likely caused by reduced *RPS2* and *RPM1* transcription (Fig. S8 G and H). Overexpression of *CPR1* also has modest effects on resistance mediated by *RPS5*, *RPS4*, *RPP2*, and *RPP4* (Fig. S7 C–F). No drastic change of transcript levels of these R genes were observed (Fig. S8 B–I).

***CPR1* Regulates the Stability of *RPS2*.** *RPS2* and *RPM1* are both CC-type NLR R proteins. *RPS2* was chosen for further testing because the *RPS2-HA* transgenic line was available to us (20) (a kind gift of B. Staskawicz, University of California at Berkeley). To test whether over-expression of *CPR1* affects the accumulation of *RPS2*, we transformed plants expressing the *RPS2-HA* fusion protein with a construct expressing *CPR1* with a C-terminal 3×FLAG tag, under its own promoter. As shown in Fig. 6C, increased expression of *CPR1*-FLAG protein correlated with reduced accumulation of *RPS2-HA*. Next we tested whether loss of *CPR1* function leads to increased accumulation of *RPS2* by crossing *cpr1-3* into the *RPS2-HA* transgenic line. Western blot analysis showed that *RPS2-HA* protein level dramatically increased in *cpr1-3* (Fig. 6D). Because *RPS2* transcript level in *cpr1-3* was only moderately higher than in wild-type (Fig. 6E), the increase in *RPS2-HA* protein level is most likely due to increased stability of *RPS2-HA* in *cpr1-3*.

A similar approach was used to test for the correlation between *CPR1* and *RPS4*, where minor effect was observed for *RPS4*-mediated immunity in *CPR1* overexpression lines (Fig. S7D). When we transformed the *RPS4-HA* transgenic line (21) (a gift of Jane Parker, MPI, Köln) with the same *CPR1*-3×FLAG construct. As shown in Fig. S9, the *RPS4-HA* level remains the same in *cpr1* and *CPR1* overexpression backgrounds as in wild-type. In contrast, when the same samples were probed with anti-*SNC1* antibody, reverse correlation between *CPR1* and *SNC1* levels was observed (Fig. S9). Thus *CPR1* does not seem to regulate *RPS4* stability.

***CPR1* Interacts with *SNC1* and *RPS2* in Vivo.** F-box proteins are known to form SCF complexes with their substrates. The genetic interaction between *CPR1* and *SNC1*, plus the negative correlations between *CPR1* protein level and accumulation of *SNC1* and *RPS2*, prompted us to test whether *CPR1* associates with *SNC1* and *RPS2* in vivo. Constructs expressing *SNC1*-HA and

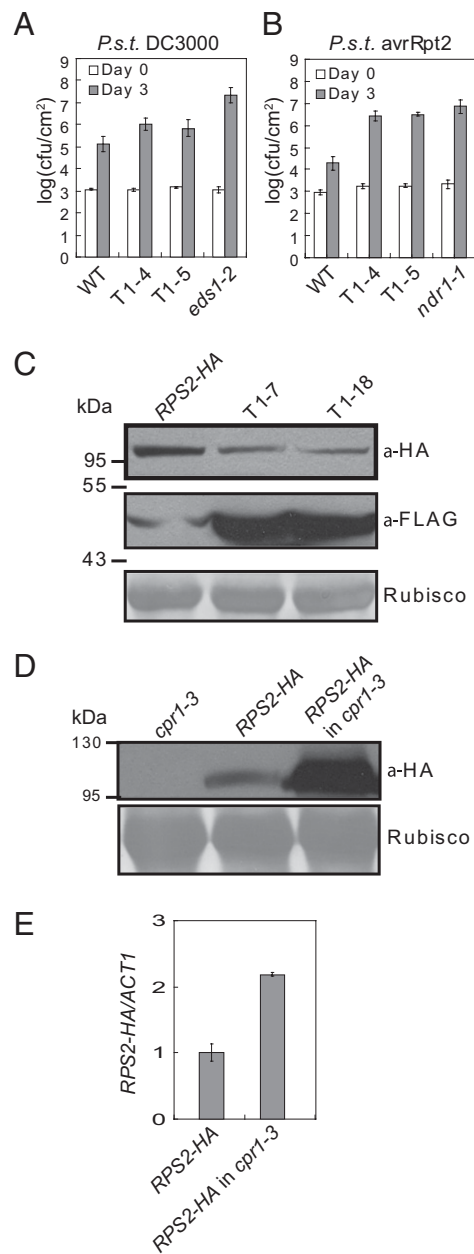


Fig. 6. Regulation of *RPS2*-mediated resistance and *RPS2* protein accumulation by *CPR1*. (A and B) Growth of *P. syringae* pv. *tomato* DC3000 (A) and *P. syringae* pv. *tomato* DC3000 carrying *avrRpt2* that is recognized by *RPS2* (B) in two independent transgenic lines (T1-4 and T1-5) overexpressing *CPR1* in wild-type Col background. WT, *eds1-2*, and *ndr1-1* plants were used as controls. (C) Western blot analysis of *RPS2-HA* protein levels in two *CPR1-FLAG* transgenic lines (T1-7 and T1-18) expressing *CPR1-FLAG* under its own promoter in a previously described *RPS2-HA* transgenic background (20). The weak band in the *RPS2-HA* lane is the result of nonspecific hybridization from anti-FLAG antibody. (D) Western blot analysis of *RPS2-HA* protein levels in *cpr1-3*. The *RPS2-HA* transgene was crossed into *cpr1-3*. (E) Expression levels of the *RPS2-HA* transgene in *RPS2-HA* and *cpr1-3* crossed into *RPS2-HA*.

CPR1-FLAG fusion proteins were cotransformed into *Arabidopsis* mesophyll protoplasts and immunoprecipitation was subsequently performed on the protein extracts using anti-FLAG agarose beads. As shown in Fig. 7A, *SNC1*-HA coimmunoprecipitated with the *CPR1*-FLAG protein. When *RPS2-HA* and *CPR1*-FLAG were coexpressed in *Arabidopsis* mesophyll proto-

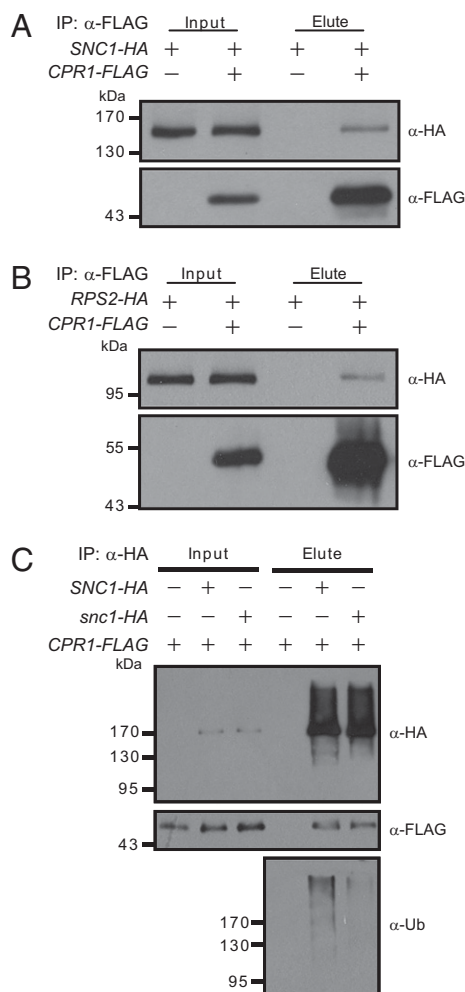


Fig. 7. Interactions between CPR1 and SNC1 (A) or RPS2 (B). (A) In vivo pull-down of SNC1-HA by CPR1-FLAG. (B) In vivo pull-down of RPS2-HA by CPR1-FLAG. (C) Immunoprecipitation of SNC1-HA or snc1-HA and ubiquitination levels of SNC1-HA or snc1-HA proteins. *Arabidopsis* mesophyll protoplasts were transfected with the indicated constructs. Total protein extracts were subjected to immunoprecipitation with anti-FLAG agarose beads (A and B) or anti-HA microbeads (C). Crude lysates (Input) and immunoprecipitated proteins (Elute) were detected with anti-FLAG, anti-HA, or anti-Ub antibodies.

plasts, RPS2-HA also coimmunoprecipitated with CPR1-FLAG (Fig. 7B). These data suggest that CPR1 does associate with SNC1 and RPS2 in vivo, probably in SCF complexes, to target SNC1 and RPS2 for degradation.

Because the point mutation in *snc1* stabilizes the SNC1 protein, we asked whether it caused a reduction of affinity with CPR1. As shown in Fig. 7C, in *Arabidopsis* mesophyll protoplasts coexpressing CPR1-FLAG and SNC1-HA or snc1-HA, when immunoprecipitation was performed on the protein extracts using anti-HA microbeads, SNC1-HA and snc1-HA are both able to pull down CPR1. The *snc1* mutation does not seem to have any obvious effect on interactions between CPR1 and SNC1 in this assay. However, when the immunoprecipitated samples were probed with an anti-ubiquitin (Ub) antibody, much less ubiquitination was observed in the immunoprecipitated snc1-HA, suggesting that SNC1 is a better substrate for ubiquitination than snc1.

Discussion

In plants, SCF-mediated protein degradation is involved in the regulation of diverse biological processes. The most well-studied

examples are from auxin signaling. SCF^{TIR1} and its homologous F-box proteins serve as auxin receptors and modulate Aux/IAA proteins for degradation (22). There is evidence that SCFs are also involved in the regulation of plant immunity. In tobacco, N-mediated resistance response to TMV was compromised when SKP1 was silenced (23). In addition, the tobacco F-box protein ACIF1 is required for the Cf-9- and Cf-4-mediated hypersensitive response, whereas the *Arabidopsis* F-box protein SON1 plays a negative role in defense (24, 25).

Recently it was shown that mutations in the F-box protein CPR30/CPR1 leads to constitutive expression of PR genes and enhanced pathogen resistance (18), but the mechanism of how CPR1 regulates plant defense responses is unclear. In this study, we provide strong evidence that SCF^{CPR1} targets the NLR R-like protein SNC1 for degradation to prevent overaccumulation of SNC1 and autoimmunity. Loss-of-function mutations in *CPR1* result in increased SNC1 accumulation, and the constitutive defense responses in *cpr1* are largely dependent on *SNC1*. In addition, overexpression of *CPR1* reduces the accumulation of SNC1 protein and suppresses the autoimmunity phenotype in *snc1*. Previously it was shown that SRFR1 and SGT1b are also involved in the negative regulation of SNC1 accumulation (11). Because SRFR1 interacts with SGT1 and SGT1 associates with SKP1 and CUL1 in vivo (7, 11, 13), SRFR1 and SGT1b may regulate the stability of SNC1 through modulating the activity of SCF^{CPR1}. In support of this hypothesis, association of SNC1 and SRFR1 was detected from coimmunoprecipitation experiments in transient expression system in tobacco (12).

In addition to SNC1, SCF^{CPR1} also negatively regulates the stability of RPS2. Loss of *CPR1* function leads to increased RPS2 levels, whereas overexpression of *CPR1* reduces the accumulation of RPS2 and severely compromises RPS2-mediated immunity. Furthermore, overexpression of *CPR1* abolishes immunity mediated by RPM1 and slightly compromises resistance specified by several other R proteins, such as RPP2 and RPP4, suggesting that SCF^{CPR1} may also target these R proteins for degradation. In contrast, overexpression of CPR1 hardly affects the resistance mediated by RPS4 and RPS5. Whether the stability of these R proteins is controlled by other F-box proteins remains to be determined. It was surprising to us that CPR1 targets SNC1 and RPS2, two quite different NLR proteins, yet doesn't target RPS4, which is more closely related to SNC1. It is possible that CPR1 may recognize a common feature shared between SNC1 and RPS2, but not with RPS4.

Previous studies on RAR1-SGT1-HSP90 demonstrated that correct folding and maintaining NLR R proteins above a threshold level are required for quick induction of defense responses when under pathogen attack. Meanwhile, the activities and protein levels of NLR R proteins need to be tightly controlled to prevent activation of defense responses without the presence of pathogens because constitutive activation of defense responses is detrimental to growth and development (7). Our study identified SCF-mediated protein degradation as a critical mechanism for regulating the stability of plant NLR R proteins, suggesting that NLR R proteins are maintained at proper levels by balanced activities from the RAR1-SGT1-HSP90-mediated assembly and proteasome-mediated degradation. Because overexpression of NLR immune receptors also results in autoactivation of immune responses in animals, and plants and animal NLRs are structurally similar, it will be interesting to test whether the stability of NLR proteins in animals is also controlled by a similar SCF-mediated mechanism.

Materials and Methods

Plant Growth Conditions and Mutant Phenotypic Characterization. All plants were grown at 22 °C under a long-day (16-h light/8-h night) regime. Gene-expression analysis was carried out by extracting total RNA from 2-wk-old plate-grown plants. The extracted RNA was then reverse-transcribed to obtain cDNA. Real-time PCR was performed and the expression levels of *Actin1*, *PR1*, and *PR2* were determined as described previously (14). Infection experiments with *P. syringae* and *H. arabidopsidis* (previously *Hyaloper-*

onospira parasitica) were performed as previously described (4). *H. arabidopsidis* infection details were visualized under a light microscope after staining leaves with lactophenol Trypan blue (26).

Construction of Plasmids and Arabidopsis Transformation. The coding sequence of *At4g12560* (*CPR1/CPR30*) was PCR-amplified using primers 5' cggGGTACCATGGCGACGATTCGAATGGA 3' and 5' CGCggatcTTATAAGAC-CAGCTTGAATC 3' from wild-type Col cDNA. The amplified fragment was then digested with KpnI and BamHI and cloned into *pHAN-35S* to generate *pHAN-35S::CPR1*. For the construction of *pCAMBIA1305-pCPR1::CPR1-3xFLAG*, the fragment containing 1,914 bp upstream of the start codon of *CPR1* and the *CPR1* genomic sequence was amplified by using primers 5' cggGGTACCaatcacaagtctactgacc 3' and 5' CGCggatcTAAGACCAGCTTG-AATCCTTGG 3' from wild-type Col genomic DNA. The fragment was digested with KpnI and BamHI and cloned into *pCAMBIA-3xFLAG* to generate *pCAMBIA1305-pCPR1::CPR1-3xFLAG*. The above plasmids were electroporated into *Agrobacterium* and subsequently transformed into the appropriate *Arabidopsis* genotypes by floral dipping method (27).

Transient expression vectors *pUC19-35S-FLAG-RBS* and *pUC19-35S-HA-RBS* (kindly provided by Jian-Min Zhou, National Institute of Biological Sciences, Beijing, People's Republic of China) containing the cauliflower mosaic virus 35S promoter, 3xFLAG or 3xHA, and a *Rubisco Small Subunit* terminator were used for transient expression of *CPR1* and R protein-coding genes in protoplasts. *CPR1*, *SNC1*, and *RPS2* coding sequences were PCR-amplified using primers listed in Table S1. The amplified fragments were digested with restriction enzymes indicated in the same table and ligated into *pUC19-35S-FLAG-RBS* or *pUC19-35S-HA-RBS*. The resulting constructs were used in the *Arabidopsis* mesophyll protoplasts transient expression system (28).

Generation of Arabidopsis Protoplasts. *Arabidopsis* mesophyll protoplasts were generated by following the protocol from Yoo et al. (28), with minor modifications. Leaf strips were digested in enzyme solution (0.4 M mannitol, 20 mM KCl, 20 mM Mes pH 5.7, 10 mM CaCl₂ and 0.1% BSA) with 1.3% cellulose R10 (Yakult Pharmaceutical Ind. Co., Ltd.) and 0.3% Macerozyme R10 (Yakult Pharmaceutical Ind. Co., Ltd.) for 2.5 h with gentle shaking. The protoplast solution was filtered through a 100- μ m nylon mesh and washed once with W5 solution (154 mM NaCl, 125 mM CaCl₂, 5 mM KCl, and 2 mM Mes pH 5.7). Isolated protoplasts were resuspended in W5 solution and incubated on ice for 30 min. After incubation, protoplasts were pelleted down and resuspended in MMG solution (0.4 M mannitol, 15 mM MgCl₂, and 4 mM Mes pH 5.7). For coimmunoprecipitation, we used 2 mL of protoplasts (in

MMG solution), 100 μ L of plasmid A (1 μ g/ μ L), 100 μ L of plasmid B (1 μ g/ μ L; or H₂O for controls), and 2.2 mL PEG solution [40% PEG4000 (Fluka; cat. no. 81240), 0.2 M mannitol and 100 mM CaCl₂]. The resulting transfection mix was well mixed and allowed to react for 10 min. The mix was then diluted with 8 mL W5 solution to stop the reaction.

Plant Total Protein Extraction, Protein Immunoprecipitation, and Western Blot Analyses. Plant total protein was extracted from 100 mg of 12-d-old plate-grown plants using extraction buffer (100 mM Tris-HCl pH 8.0, 0.2% SDS and 2% β -mercaptoethanol). Laemmli buffer (4x) was added to each protein sample and boiled for 5 to 10 min. The resulting protein samples were subjected to Western blot analyses.

For protein immunoprecipitation, proteins in the transfected protoplasts were extracted using 1.5 mL grinding buffer [50 mM Tris-HCl pH 7.5, 10 mM MgCl₂, 150 mM NaCl, 0.1% Nonidet P-40, 1 mM PMSF, 1x Protease Inhibitor Cocktail (Roche; Cat. #11873580001), and 100 μ M MG132]. The sample was spun at 16,000 \times g for 10 min at 4 $^{\circ}$ C to remove cellular debris. Forty microliters of the supernatant was saved as input. The rest of the supernatant was transferred to a tube containing 35 μ L anti-FLAG M2 beads (Sigma; Cat. #A2220) and incubated for 2 h at 4 $^{\circ}$ C with gentle rotation. After incubation, the beads were spun down at 1,500 \times g for 30 s at 4 $^{\circ}$ C. The beads were washed thoroughly with 1 mL of grinding buffer three times before immunoprecipitated proteins were eluted with 60 μ L 3 \times FLAG peptide (150 μ g/mL; Sigma, Cat. #F4799).

The anti-SNC1 antibody was generated against a SNC1-specific peptide in rabbit (11). The anti-HA antibody was from Roche (Cat. #11867423001). The anti-FLAG antibody and the anti-Ubiquitin antibody were both from Sigma (Cat. #F1804 and U0508, respectively).

ACKNOWLEDGMENTS. We thank our colleagues around the globe who kindly provided us with materials: Dr. Judy Callis for seeds of the *cul1-7* and transgenic *CUL1-FLAG* in *cul1-7*; Dr. Jian-Min Zhou for *pUC19-35S-FLAG-RBS* and *pUC19-35S-HA-RBS*; Dr. Brian Staskawitz for seeds of the *RPS2-HA* transgenic line; Dr. Jane Parker for seeds of the *RPS4-HA* transgenic line; Dr. Guoying Wang for seeds of *cpr1-2* (previously *cpr30-1*) and *cpr1-2 pad4*; Dr. Mary Beebe and Dr. Sean Graham for their help with phylogenetic analysis of *CPR1* and its homologs; Kaeli Johnson and Virginia Woloshen for careful reading of the manuscript; and Yan Li for assistance with making figures. Work described is supported by funds from Natural Sciences and Engineering Research Council of Canada (to X.L.) and the Chinese Ministry of Science and Technology (to Y.Z.).

- Jones JD, Dangl JL (2006) The plant immune system. *Nature* 444:323–329.
- Eitas TK, Dangl JL (2010) NB-LRR proteins: Pairs, pieces, perception, partners, and pathways. *Curr Opin Plant Biol* 13:472–477.
- Magalhaes JG, Sorbara MT, Girardin SE, Philpott DJ (2011) What is new with Nods? *Curr Opin Immunol* 23(1):29–34.
- Li X, Clarke JD, Zhang Y, Dong X (2001) Activation of an EDS1-mediated R-gene pathway in the *snc1* mutant leads to constitutive, NPR1-independent pathogen resistance. *Mol Plant Microbe Interact* 14:1131–1139.
- Shirano Y, Kachroo P, Shah J, Klessig DF (2002) A gain-of-function mutation in an *Arabidopsis* Toll Interleukin1 receptor-nucleotide binding site-leucine-rich repeat type R gene triggers defense responses and results in enhanced disease resistance. *Plant Cell* 14:3149–3162.
- Tan X, et al. (2007) Global expression analysis of nucleotide binding site-leucine rich repeat-encoding and related genes in *Arabidopsis*. *BMC Plant Biol* 7:56.
- Shirasu K (2009) The HSP90-SGT1 chaperone complex for NLR immune sensors. *Annu Rev Plant Biol* 60:139–164.
- Zhang M, Kadota Y, Prodromou C, Shirasu K, Pearl LH (2010) Structural basis for assembly of Hsp90-Sgt1-CHORD protein complexes: Implications for chaperoning of NLR innate immunity receptors. *Mol Cell* 39:269–281.
- Mayor A, Martinon F, De Smedt T, Pétrilli V, Tschopp J (2007) A crucial function of SGT1 and HSP90 in inflammasome activity links mammalian and plant innate immune responses. *Nat Immunol* 8:497–503.
- Holt BF, 3rd, Belkhadir Y, Dangl JL (2005) Antagonistic control of disease resistance protein stability in the plant immune system. *Science* 309:929–932.
- Li Y, et al. (2010) SRFR1 negatively regulates plant NB-LRR resistance protein accumulation to prevent autoimmunity. *PLoS Pathog* 6:e1001111.
- Kim SH, et al. (2010) The *Arabidopsis* resistance-like gene *SNC1* is activated by mutations in SRFR1 and contributes to resistance to the bacterial effector AvrRps4. *PLoS Pathog* 6:e1001172.
- Azevedo C, et al. (2002) The RAR1 interactor SGT1, an essential component of R gene-triggered disease resistance. *Science* 295:2073–2076.
- Zhang Y, Goritschnig S, Dong X, Li X (2003) A gain-of-function mutation in a plant disease resistance gene leads to constitutive activation of downstream signal transduction pathways in *suppressor of npr1-1, constitutive 1*. *Plant Cell* 15:2636–2646.
- Wiermer M, Feys BJ, Parker JE (2005) Plant immunity: The EDS1 regulatory node. *Curr Opin Plant Biol* 8:383–389.
- Shen WH, et al. (2002) Null mutation of *AtCUL1* causes arrest in early embryogenesis in *Arabidopsis*. *Mol Biol Cell* 13:1916–1928.
- Gilkerson J, et al. (2009) Isolation and characterization of *cul1-7*, a recessive allele of *CULLIN1* that disrupts SCF function at the C terminus of CUL1 in *Arabidopsis thaliana*. *Genetics* 181:945–963.
- Gou M, et al. (2009) An F-box gene, CPR30, functions as a negative regulator of the defense response in *Arabidopsis*. *Plant J* 60:757–770.
- Bowling SA, et al. (1994) A mutation in *Arabidopsis* that leads to constitutive expression of systemic acquired resistance. *Plant Cell* 6:1845–1857.
- Axtell MJ, Staskawicz BJ (2003) Initiation of RPS2-specified disease resistance in *Arabidopsis* is coupled to the AvrRpt2-directed elimination of RIN4. *Cell* 112:369–377.
- Wirthmueller L, Zhang Y, Jones JDG, Parker JE (2007) Nuclear accumulation of the *Arabidopsis* immune receptor RPS4 is necessary for triggering EDS1-dependent defense. *Curr Biol* 17:2023–2029.
- Santner A, Estelle M (2009) Recent advances and emerging trends in plant hormone signalling. *Nature* 459:1071–1078.
- Liu Y, Schiff M, Serino G, Deng XW, Dinesh-Kumar SP (2002) Role of SCF ubiquitin-ligase and the COP9 signalosome in the N gene-mediated resistance response to *Tobacco mosaic virus*. *Plant Cell* 14:1483–1496.
- van den Burg HA, et al. (2008) The F-box protein ACRE189/ACIF1 regulates cell death and defense responses activated during pathogen recognition in tobacco and tomato. *Plant Cell* 20:697–719.
- Kim HS, Delaney TP (2002) *Arabidopsis* SON1 is an F-box protein that regulates a novel induced defense response independent of both salicylic acid and systemic acquired resistance. *Plant Cell* 14:1469–1482.
- Koch E, Slusarenko A (1990) *Arabidopsis* is susceptible to infection by a downy mildew fungus. *Plant Cell* 2:437–445.
- Clough SJ, Bent AF (1998) Floral dip: A simplified method for *Agrobacterium*-mediated transformation of *Arabidopsis thaliana*. *Plant J* 16:735–743.
- Yoo SD, Cho YH, Sheen J (2007) *Arabidopsis* mesophyll protoplasts: A versatile cell system for transient gene expression analysis. *Nat Protoc* 2:1565–1572.